

Role of Initial Conditions in Establishing Asymptotic Flow Behavior

William K. George* and Lars Davidson†
Chalmers University of Technology, SE-412 96 Gothenburg, Sweden

The role of the details of initial (or upstream) conditions in establishing asymptotic behavior is reviewed. The traditional view that at least simple shear flows reach universal asymptotic states is shown to be inconsistent with the abundant experimental and direct-numerical-simulation data. Even though scaled mean velocity profiles collapse, the streamwise (or temporal) variation of the scaling parameters and spreading rates can vary widely for different upstream (or initial) conditions. Equilibrium similarity theory shows why the traditional view has arisen: normalized mean velocity profiles can be universal, even though the other moment profiles and scaling parameters are not. Decaying isotropic turbulence and applications of the proper orthogonal decomposition to free shear flows are used to show what parameters might control the downstream development. It is argued that Reynolds-averaged Navier–Stokes cannot account for these dependencies, but large-eddy simulation can.

Nomenclature

C_q = coefficient for energy spectrum function near $k = 0$
 C_{ϵ_2} = coefficient in dissipation equation, Eq. (25)
 C_μ = coefficient of eddy viscosity, $C_\mu = \nu_t/(U_s \delta)$
 D = jet or disk diameter
 D_u = scale function for dissipation defined by Eq. (7)
 d_u = profile function for dissipation defined by Eq. (7)
 E = three-dimensional energy spectrum function for isotropic turbulence,

$$\frac{3\langle u^2 \rangle}{2} = \int_0^\infty E(k, t) dk$$

E_s = time-dependent scale function for $E(k, t)$ defined by Eq. (17)
 F = dimensionless three-dimensional spectral energy spectrum function defined by Eq. (17)
 f = frequency, Hz
 \tilde{f} = mean velocity profile function defined by Eq. (2)
 G = dimensionless three-dimensional spectral energy transfer defined by Eq. (18)
 g = Reynolds shear-stress profile function defined by Eq. (3)
 \tilde{g} = renormalized Reynolds shear-stress profile function defined by Eq. (14)
 K_u = scale function for $\langle u^2 \rangle$ defined by Eq. (4)
 k = wave number
 \bar{k} = dimensionless wave number defined by $\bar{k} = kl(t)$
 k_u = profile function for $\langle u^2 \rangle$ defined by Eq. (4)
 l = time-dependent length scale for decaying turbulence, proportional to Taylor microscale, λ
 M = highest resolved azimuthal proper-orthogonal-decomposition (POD) mode
 m = azimuthal mode number in POD eigenspectra
 n = exponent for temporal decay of turbulence energy, $3\langle u^2 \rangle/2 \propto t^{-n}$
 P = mean pressure

P_u = pressure strain-rate scale function defined by Eq. (6)
 p = fluctuating pressure
 p_u = pressure strain-rate profile function defined by Eq. (6)
 q = exponent for wave-number dependence near $k = 0$
 R_s = Reynolds shear-stress scaling function defined by Eq. (3)
 r = radial coordinate
 T = three-dimensional spectral energy transfer function
 T_s = time-dependent scale function for $T(k, t)$ defined by Eq. (18)
 T_{u^2v} = scale function defined by Eq. (5)
 t = time
 t_{u^2v} = profile function defined by Eq. (5)
 U = mean streamwise velocity
 U_{CL} = centerline velocity
 U_s = mean velocity scale function defined by Eq. (2), usually chosen as U_0
 U_0 = centerline velocity deficit
 U_∞ = freestream velocity
 u = fluctuating streamwise velocity
 v = fluctuating radial velocity
 x = streamwise coordinate
 δ = local shear-layer thickness (usually δ_*)
 δ_* = choice of δ so that integral in Eq. (11) equals unity
 ϵ = rate of dissipation per unit volume of turbulence energy
 η = normalized radial coordinate, $\eta = r/\delta$
 θ = momentum thickness defined by

$$\int_0^\infty U(U_\infty - U)r dr \approx U_\infty \int_0^\infty (U_\infty - U)r dr$$

for far wake

λ = Taylor microscale, for isotropic turbulence
 $\lambda^2 = 15\nu\langle u^2 \rangle/\epsilon$
 $\lambda^{(1)}$ = first radial POD eigenspectrum from POD integral equation
 ν = kinematic viscosity
 ν_t = turbulence eddy viscosity defined by Eq. (21)
 $\xi^{(1)}$ = eigenspectrum $\lambda^{(1)}(f, m; x)$ normalized by energy in all azimuthal modes, m

Presented as Paper 2003-0064 at the AIAA 41st Aerospace Sciences Meeting, Reno, NV, 6–9 January 2003; received 30 June 2003; revision received 12 October 2003; accepted for publication 23 October 2003. Copyright © 2003 by the American Institute of Aeronautics and Astronautics, Inc. All rights reserved. Copies of this paper may be made for personal or internal use, on condition that the copier pay the \$10.00 per-copy fee to the Copyright Clearance Center, Inc., 222 Rosewood Drive, Danvers, MA 01923; include the code 0001-1452/04 \$10.00 in correspondence with the CCC.

*Professor, Department of Thermo and Fluid Dynamics. Member AIAA.

†Professor, Department of Thermo and Fluid Dynamics.

Introduction

ONE of the most persistent ideas from the past century of turbulence research is that turbulence “forgets” its initial conditions. Indeed, most mean velocity profiles of simple free shear flows collapse when plotted using a velocity scale and an appropriately defined width. For example, the normalized mean velocity profiles

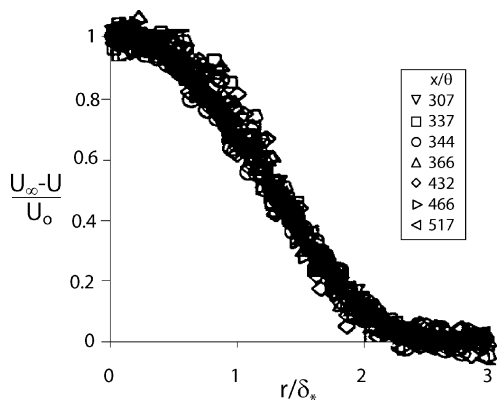


Fig. 1 Mean velocity profiles for the porous disk with $\sigma = 0.70$; data of Cannon¹ (from Ref. 2).

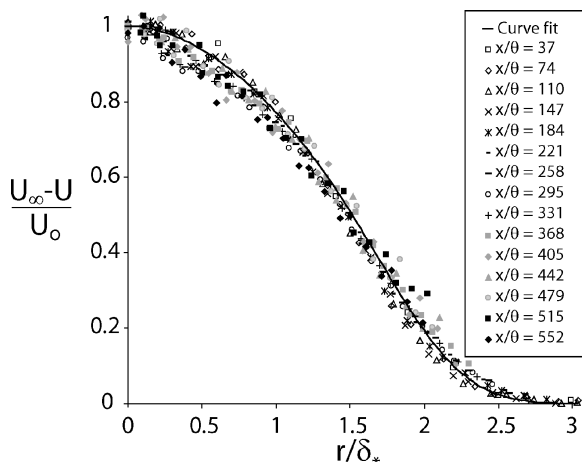


Fig. 2 Mean velocity profiles for disk; data of Johansson³ (from Ref. 2).

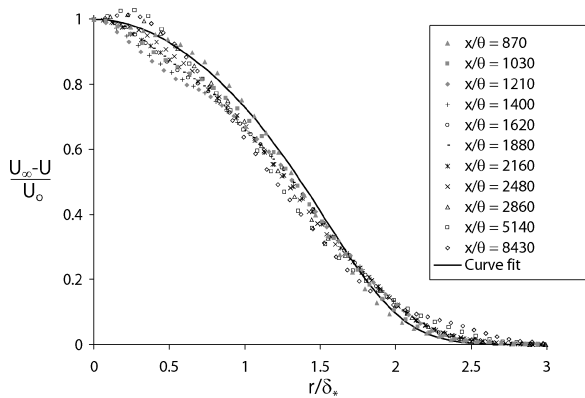


Fig. 3 Mean velocity profiles for the DNS high-Reynolds-number wake; data of Gourlay et al.⁴ fitted in Fig. 2 to the data of disk wake profile of Johansson³ (from Ref. 2).

shown in Figs. 1–3^{1–4} for the far axisymmetric wake (in a uniform external stream) from a variety of wake generators [including those used in direct numerical simulation (DNS)] all collapse to virtually the same curve, seemingly independent of initial (or upstream) conditions.²

Plots like this are shown in most texts and cited as evidence for asymptotic independence of initial conditions. What is often not shown, even in many of the original journal papers, is the differing streamwise dependence of the normalizing (or scaling) parameters from experiment to experiment or from one source to another. Figure 4 shows the wake widths (the normalization length scale for the preceding plots) for the same experiments shown in Figs. 1–3, along with a number of other experiments. Clearly the spreading rates of these wakes depend dramatically on the initial conditions to distances very far downstream and by amounts that cannot be simply

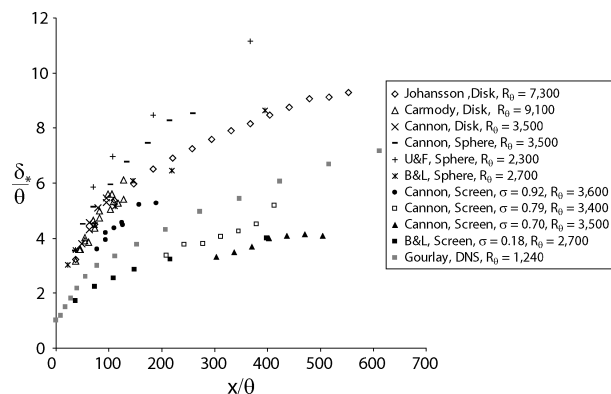


Fig. 4 Cross-stream length scale δ_s/θ vs x/θ . For the screen wakes, the porosity σ is defined as $\sigma = (\text{solid area})/(\text{total area})$ (from Johansson et al.²).

attributed to experimental error. This is contrary to the conventional wisdom, and so either the traditional view must be wrong, or it hardly provides useful information because the transients persist so far downstream.

This paper will briefly attempt to assess what we know at present about the role initial conditions play in turbulence. Our focus is not on large-eddy simulations (LES) per se but rather to review our current understanding of the underlying physics. Our hope is that this will contribute to a better understanding of how to use LES for real problems, and as well stimulate its use to explore further these phenomena.

How Can Some Profiles Be Independent of Initial Conditions, and Others Not?

Given the long history of turbulence, it is not enough to simply state that a previously believed idea is wrong, or even that another idea is better. Instead it is necessary to show why it came to be believed in the first place. The point of this section is to outline briefly how this happened and in the process show what was overlooked.

There are numerous experiments and computer simulations over the past decade and a half that confirm the apparent asymptotic dependence of the spreading rate of free shear flows on the initial conditions. These include Wygnanski et al.⁵ (experiments in plane wakes), Grinstein et al.,⁶ Grinstein⁷ (DNS and LES of jets), Ghosal and Rogers⁸ (LES of wakes), Boersma et al.⁹ (DNS of jets), Mi et al.¹⁰ (experiments in jets), and Slessor et al.¹¹ (experiments in shear layers), to cite but a few. The wake experiments used different wake generators, the jets different exit conditions, and the LES and DNS different forcing of the largest scales. Although the variations in jet spreading rate were on the order of 20% typically, it was possible to make dramatic differences in the wakes (several hundred percent or more). There is even some evidence that the outer part of turbulent boundary layers retains a dependence on its upstream conditions.^{12–14}

As will be discussed next, it is not clear at this time precisely how or why the initial conditions can be preserved asymptotically. It has been clear since George,^{15,16} however, that equilibrium similarity analysis can account for this behavior. In other words, there is no conflict between properly done similarity theory and these results. The initial conditions simply show up in the spreading rate and the undetermined coefficients. Most importantly, if the Reynolds stress and mean velocity are properly normalized the mean momentum equation is independent of all parameters. For example, for the high-Reynolds-number axisymmetric wake in a constant velocity external flow (compare Ref. 2) the momentum equation in similarity variables reduces to

$$\left[\frac{\delta}{U_s} \frac{dU_s}{dx} \right] \tilde{f} - \left[\frac{d\delta}{dx} \right] \eta \tilde{f}' = \left[\frac{R_s}{U_\infty U_s} \right] \frac{1}{\eta} \frac{d}{d\eta} \eta g \quad (1)$$

where any single point moment is assumed to be expressible as a product of two functions; that is,

$$U - U_\infty = U_s(x, *)\tilde{f}(\eta, *) \quad (2)$$

$$-\langle uv \rangle = R_s(x, *)g(\eta, *) \quad (3)$$

$$\frac{1}{2}\langle u^2 \rangle = K_u(x, *)k_u(\eta, *) \quad (4)$$

$$\frac{1}{2}\langle u^2 v \rangle = T_{u^2v}(x, *)t_{u^2v}(\eta, *) \quad (5)$$

$$\left\langle \frac{p}{\rho} \frac{\partial u}{\partial x} \right\rangle = P_u(x, *)p_u(\eta, *) \quad (6)$$

$$\epsilon_u = D_u(x, *)d_u(\eta, *) \quad (7)$$

$$\text{etc.} \quad (8)$$

and where $\eta = r/\delta(x, *)$ and the $*$ denotes a possible (but unknown) dependence on initial (or upstream) conditions. (This is not restrictive because if it is not possible no solutions will be found.) U_s can be taken to be the centerline velocity deficit U_0 , and δ can be taken as the δ_* defined later with no loss of generality.

Thus we are seeking solutions to transformed versions of the momentum (and Reynolds-stress equations as well) for which the bracketed terms are functions of only the streamwise variable x and the upstream conditions, and the functions outside the square brackets are functions of only the similarity variable η and possibly the initial conditions. We have allowed each term entering the equations to have its own scaling function, and we have not specified them arbitrarily nor by ad hoc arguments. For example, we have not taken $R_s(x) = U_s(x)^2$, etc., as in most texts.

Now the question we ask is, do there exist solutions to these transformed equations (or subsets of them) for which all of the terms in square brackets have exactly the same dependence on x ? If so, we call these equilibrium similarity solutions. It is clear they must be the asymptotic solution because if any term has a different x dependence it will either dominate or die off leaving a different set of equations. For our example, equilibrium similarity requires

$$\left[\frac{\delta}{U_s} \frac{dU_s}{dx} \right] \propto \left[\frac{d\delta}{dx} \right] \propto \left[\frac{R_s}{U_\infty U_s} \right] \quad (9)$$

This implies that an equilibrium similarity solution is possible only if the scale for $-\langle uv \rangle$ is

$$R_s \propto U_\infty U_s \frac{d\delta}{dx} \quad (10)$$

It is also straightforward to show that Eq. (10) implies U_s must be proportional to a power of δ —but not necessarily a power of x , contrary to the assumption of most texts. The explicit x dependence can only be found by consideration of the higher moment equations (compare George^{15,16} or for this problem Johansson et al.²).

Almost every problem has some kind of integral constraint; for this one the net momentum deficit must equal the drag. Far downstream this implies that

$$U_\infty U_s \delta^2 \int_0^\infty \tilde{f} \eta d\eta = U_\infty^2 \theta^2 \quad (11)$$

Note that δ_* is defined as the choice of δ , which makes the integral unity. Because the integral can at most depend on the initial (or upstream) conditions, it follows from differentiation that

$$\frac{\delta}{U_s} \frac{dU_s}{dx} = -2 \frac{d\delta}{dx} \quad (12)$$

Substitution into Eq. (1) yields

$$-2\tilde{f} - \eta\tilde{f}' = \left[\frac{R_s}{U_\infty U_s d\delta/dx} \right] \frac{1}{\eta} \frac{d}{d\eta} \eta g \quad (13)$$

But this can be reduced even further by incorporating the scale factor $R_s/(U_\infty U_s d\delta/dx) = \text{constant}$ into g by defining

$$\tilde{g} = \left[\frac{R_s}{U_\infty U_s d\delta/dx} \right] g \quad (14)$$

from which it follows that the momentum equation reduces to

$$-\frac{d}{d\eta} \eta^2 \tilde{f} = \frac{d}{d\eta} \eta \tilde{g} \quad (15)$$

Thus the final scaled momentum equation is entirely independent of the source conditions, no matter how much the scaling parameters themselves depend on them.

Because the scaled mean velocity and Reynolds-stress profiles are the solution to Eq. (15), obviously they must be independent of source conditions as well. By contrast, the scaling parameters U_0 and $R_s = U_\infty U_s d\delta/dx$ can still depend on source conditions (and from all evidence do). The Reynolds stress is especially interesting because it is normalized by some combination of velocity squared times the growth rate $d\delta/dx$ (instead of just the U_s^2 found in most journal articles and texts). Thus the Reynolds-stress profile is the same for all wakes, but its amplitude depends on the initial conditions. It is this incorporation of the growth rate into the Reynolds-stress scaling that removes the source conditions from the transformed momentum equation.

As first noted by George,¹⁵ this absorption of the initial condition dependent parameters can usually only be done for the mean momentum equation and not for the higher moment equations. Thus the higher moment profiles can vary from one set of initial conditions to another. Interestingly, all of the normal stresses $\langle u^2 \rangle$, $\langle v^2 \rangle$, and $\langle w^2 \rangle$ can be shown to scale with U_s^2 , but all of the transverse transport moments involve $d\delta/dx$ (like $\langle uv \rangle$, which scales with $U_\infty U_s d\delta/dx$ instead of simply U_s^2). The same is also true for the third moments where the lateral transport moments all involve $d\delta/dx$. Physically this makes sense because it is the lateral transport of momentum and energy that allows the flow to spread. If the spreading rate depends on the initial conditions, then so must the scaling parameters for these moments—and they do.

Equilibrium similarity has been discussed in detail in a variety of places in addition to the 1989 and 1995 references, for example, Moser et al.,¹⁷ Rogers,¹⁸ Johansson et al.,² George et al.,¹² and Castillo and George.^{13,19} The important point to be drawn from the discussion here is that in every case the result is the same: the scaled momentum equation implies that the properly scaled mean velocity and Reynolds-stress profiles are always independent of the initial (or source) conditions, but scaling parameters and other moment profiles are not. Thus collapse of some profiles (like mean velocity) has nothing to do with whether the turbulence retains a dependence on initial conditions. Instead it is an artifact of the choice of scales and the momentum equation itself. But it was precisely this universality of such mean profiles that led the turbulence community to accept the idea of independence from initial conditions in the first place, clearly a logical fallacy. And it was the erroneous assumption that all moments could be scaled by a single length and velocity scale (self-preservation) that seemed to justify it.

Homogeneous Turbulence Remembers Too

The asymptotic dependence on initial conditions is not confined to the single-point Reynolds-averaged Navier–Stokes (RANS) equations of turbulent free shear flows but characterizes the multipoint equations as well (e.g., George,²⁰ George and Gibson,²¹ Ewing,²² and Ewing and George²³). For example, equilibrium similarity theory can be applied to the spectral energy equation of decaying isotropic turbulence:

$$\frac{\partial E}{\partial t} = T - 2\nu k^2 E \quad (16)$$

where $E(k, t)$ is the three-dimensional spectrum function and $T(k, t)$ is the nonlinear spectral transfer function. George²⁰ was

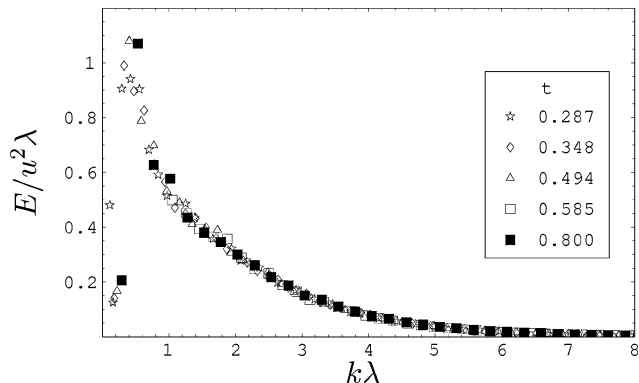


Fig. 5 $E(k)/u^2\lambda$ vs $k\lambda$ for the de Bruyn Kops and Riley²⁴ DNS data (from Wang and George²⁵).

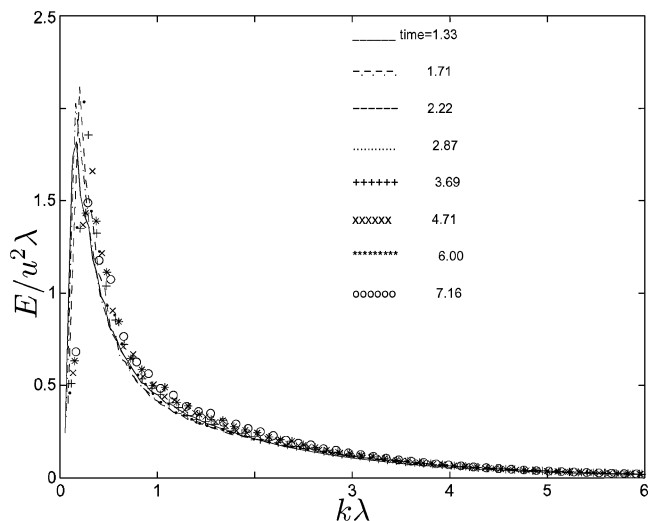


Fig. 6 $E(k)/u^2\lambda$ vs $k\lambda$ for the Wray²⁶ DNS data (from Wang and George²⁵).

able to deduce that equilibrium similarity solutions were possible of the form

$$E(k, t) = E_s(t, *)F(\bar{k}, *) \tag{17}$$

$$T(k, t) = T_s(t, *)G(\bar{k}, *) \tag{18}$$

where $\bar{k} = kl(t)$ and $l(t)$ could be either the integral scale or the Taylor microscale (because their ratio was constant during decay). Figures 5 (Refs. 24 and 25) and 6 (Refs. 25 and 26) from the paper by Wang and George²⁵ show such collapse for the data from two recent 512³ DNS for decaying turbulence using the deduced scales $E_s = \langle u^2 \rangle \lambda$ and $T_s = \nu \langle u^2 \rangle / \lambda$.

The theory also deduces that the energy should decay as a power law in time $3\langle u^2 \rangle / 2 \propto t^{-n}$, where the constant decay exponent $n(*)$ could possibly depend on the initial conditions. For all data sets considered (including the experimental data of Comte-Bellot and Corrsin^{27,28}), it did.

The nondimensional nonlinear spectral transfer term $G(\bar{k})$ is also invariant during decay and depends uniquely on the decay exponent n and the energy spectrum $F(\bar{k})$. It is straightforward to show that equilibrium similarity applied to Eq. (16) yields

$$G = \{[5/n](\bar{k}F' + F) - 10F\} + 2\bar{k}^2F \tag{19}$$

Figure 7 taken from George and Wang²⁹ shows the nonlinear spectral transfer for a single time ($R_\lambda = 50$) from the DNS simulation of Wray²⁶ and that calculated from Eq. (19) using the energy spectrum function and the value of $n = 1.5$ determined from the energy decay rate by Wang and George.²⁵ Also shown separately are the dissipation and temporal decay spectra, the latter of which is clearly not negligible as often assumed. Figure 8, also from George and Wang,²⁹ shows the same calculation for the high-Reynolds-number experiment ($R_\lambda = 237$) of Helland et al.³⁰ at a single downstream distance from a grid using $n = 1$. The value of n is crucial in both figures in determining the low wave-number behavior and locating the minimum value.

Figure 9 (from George²⁰) suggests strongly that the decay exponent for turbulence behind grids depends mostly on the Reynolds number of the grid. In fact, there is no evidence that the turbulence ever evolves into the so-called final period of decay for which $n = 5/2$, but rather it decays this way when the Reynolds number of

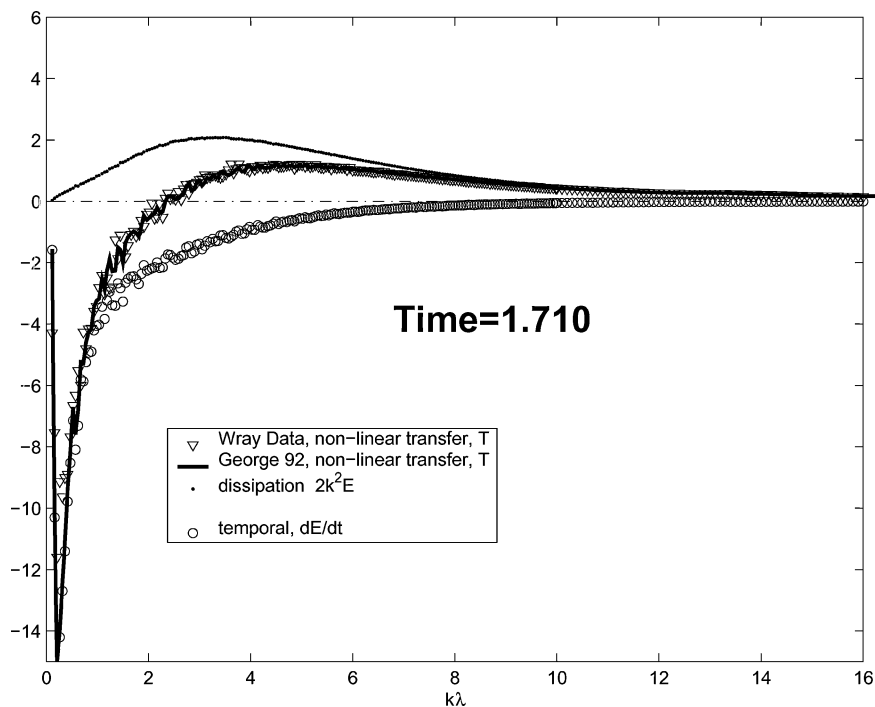


Fig. 7 DNS data of Wray²⁶ for $\lambda T/\nu u^2$ vs $k\lambda$ with terms calculated from similarity equation (19) using measured spectrum: $n = 1.5$ and $R_\lambda = 50$ (from George and Wang²⁹).

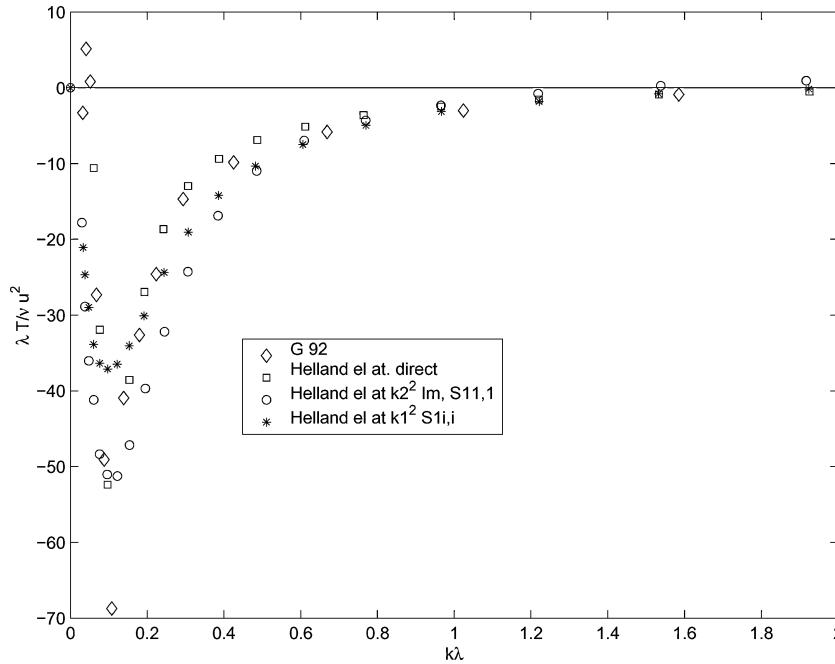


Fig. 8 Experimental data of Helland et al.³⁰ for $\lambda T/\nu u^2$ vs $k\lambda$ with similarity equation (19) using measured spectrum: $n = 1$ and $R_\lambda = 237$ (from George and Wang²⁹).

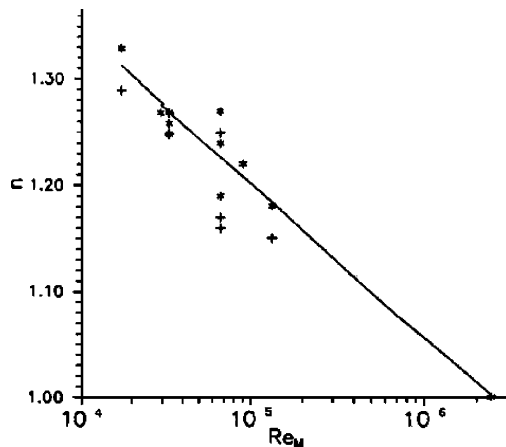


Fig. 9 Dependence of grid turbulence decay exponent on grid Reynolds number (from George²⁰).

the grid is very low. Note that the value of n is constant throughout decay, and departures from constant n are most likely caused by box size effects as the scales grow too large for the experimental or computational domain (compare Wang and George²⁵).

Much stronger variation of n with initial conditions has been observed for DNS (e.g., Wray and Mansour,³¹ and Wang and George²⁵). In fact, for at least the modest to low Reynolds numbers of the DNS and experiments the exponent n appears to be determined by the very lowest wave numbers of the spectrum, which can be invariant (in physical variables) during decay. In particular, if $E(k, t) = C_q k^q$ for small k and is invariant during decay, then

$$n = (q + 1)/2 \quad (20)$$

The current thinking is that $0 < q \leq 4$, corresponding to $1/2 < n \leq 5/2$. (Note that there is no reason to assume q to be integer, nor the spectrum to be analytical for small k .) The recent shell-model simulations of M. V. Melander (private communication to W. K. George, 2002) support the overall equilibrium similarity, but suggest strongly that Eq. (20) is only valid for relatively small values of R_λ (perhaps $R_\lambda < 100$). Clearly this means the lowest wave numbers are not invariant (in physical variables) at high initial Reynolds numbers but are at low initial Reynolds numbers. Although we do not yet completely understand this, it is consistent with the observa-

tion for grid turbulence that the value of n diminishes toward unity as the grid Reynolds number is increased.

Does It Matter That Turbulence Can Remember?

At first sight it might seem that it does not matter. After all, we are simply solving differential equations, and of course we should expect them to depend on the initial and boundary conditions. Actually the question is of considerable importance both to LES and the study of turbulence in general. If inlet boundary conditions uniquely determine the asymptotic solution, without this knowledge we have no idea how to choose them other than blindly. But there is an even more serious problem, first noted by Taulbee³² and George,¹⁵ both in the same volume. Single-point turbulence models (RANS) are missing the necessary physics to be able to account for these asymptotic effects of the initial conditions. This is most easily illustrated by two examples.

Example 1: Simple Eddy Viscosity

First consider a simple eddy viscosity that relates Reynolds stress to the mean velocity gradient for the wake just considered, say,

$$\langle -uv \rangle = \nu_t \frac{\partial U}{\partial r} \quad (21)$$

where we will take $\nu_t = C_\mu U_s \delta$.

In similarity variables this becomes

$$[R_s]g = \left[\frac{\nu_t U_s}{\delta} \right] \frac{df}{d\eta} \quad (22)$$

As before all of the x dependence is in the square brackets. Using $R_s = U_\infty U_s \delta d\delta/dx$, it is clear that ν_t must satisfy the following:

$$\nu_t = C_\mu U_s \delta \propto U_\infty \delta \frac{d\delta}{dx} \quad (23)$$

But we know $d\delta/dx$ depends on the initial conditions. Hence the initial conditions that affect the asymptotic growth rate show up in the worst possible place: the modeling coefficient.

It is easy to show that the same line of reasoning applies to any kind of gradient closure. For example, if we take $\langle -u^2 v \rangle \propto \partial(u^2)/\partial r$ the same problem occurs: we end up with our modeling coefficient proportional to $d\delta/dx$. Thus even if the model predicts exactly the right dimensionless profile (and it usually does), the spreading rate is entirely determined by the model coefficients. And these are in turn determined by some unspecified (and as yet unknown) source conditions.

Example 2: Isotropic Decaying Turbulence

It is straightforward to show that for the isotropic decaying turbulence just considered equilibrium similarity implies directly (without additional assumptions) so that

$$\frac{3}{2} \frac{d\langle u^2 \rangle}{dt} = -\epsilon \tag{24}$$

and surprisingly,

$$\frac{d\epsilon}{dt} = -\left[\frac{n+1}{n} \right] \frac{\epsilon^2}{3\langle u^2 \rangle / 2} = -C_{\epsilon_2} \frac{\epsilon^2}{3\langle u^2 \rangle / 2} \tag{25}$$

where $3\langle u^2 \rangle / 2$ is the kinetic energy and n is the constant power law exponent. Thus equilibrium similarity yields exactly the familiar $k-\epsilon$ model, but as an exact result and not a just model. Moreover the coefficient C_{ϵ_2} in the ϵ equation is uniquely determined by the decay exponent n , which appears to be dependent on the initial conditions. In this case, however, we have a clue that it depends on the initial spectrum at the lowest wave numbers (at least at low Reynolds numbers) [Eq. (20)]. If so, then our RANS model can be exact, but it is virtually useless because there is nothing in the RANS equations to determine the unknown q (or n) without specifying it in advance.

But Does Not LES Have the Same Problem?

Actually the answer appears to be no. LES, whether in space variables or wave-number variables, resolves the largest scales (or lowest wave numbers) exactly, at least within the limitations of the box size (or lowest wave number). And it seems to be these large scales that preserve (or dictate) the most important initial conditions. Two examples illustrate this.

The first is the example of isotropic decaying turbulence just shown. If the overall decay rate is truly determined by the lowest wave numbers (at least for modest Reynolds numbers), then it is precisely these that the LES keeps. Clearly this puts substantial computational constraints on the ratio of the energetic scales to these very large scales, perhaps like those noted by Wang and George²⁵ for ratio of size of the integral scale to the size of the domain. (Note that similar constraints were noted by Grinstein³³ for jets.) Obviously unphysical backscatter from the closure model can also have a detrimental effect.

The second example is the LES simulation of the time-dependent wake by Ghosal and Rogers⁸ just cited. They first showed they could duplicate the DNS results reported by Moser et al.¹⁷ for the unforced time-dependent wake. Then they showed by applying varying amounts of forcing to the largest scale they could vary the asymptotic growth rate substantially (by a factor of 5), all of the while maintaining equilibrium similarity (at least until effects of the finite domain manifest themselves).

More tangible evidence of the relation of the large scales to LES is provided by the paper in this same volume by Druault et al.³⁴ Turbulence for a free shear layer (from experiments and DNS) is first characterized by proper-orthogonal-decomposition (POD) techniques, then these POD results are used to generate with some success initial conditions for LES. Because the lower-order POD modes are dominated by the largest and most energetic structures, clearly this is what the LES needs. But why?

How Does Turbulence Remember?

From the preceding examples it is clear, both in principle and in practice, that LES contains the “necessary physics” to produce an asymptotic dependence on initial conditions. Similarly it is clear that RANS does not. Even though the RANS models might have exactly the right functional dependence, the fact that the initial conditions appear in the coefficients renders them fundamentally flawed. In particular, no general set of universally valid parameters should be expected. Note that this, of course, does not preclude their careful use for engineering purposes, especially where empirical knowledge is built into these coefficient choices. This is, of course, exactly what we have learned from three decades of RANS use.

But what is this necessary physics? Obviously it must be related to vorticity production, convection, and diffusion. But word descriptions of what is happening alone are not enough to explain how the effects can persist far downstream. There must be some quantitative means by which whatever structures there are can be both described and continuously regenerated and in a manner that retains some of the initial conditions. How this might happen poses very difficult questions to which we are just beginning to find clues. Some come from the recent POD studies of Delville et al.,³⁵ Citriniti and George,³⁶ Gordeyev and Thomas,³⁷ Ukeiley et al.,³⁸ Jung et al.,³⁹ Johansson et al.,⁴⁰ Gamard et al.,⁴¹ and George et al.,⁴² among others. These allow a detailed examination of how the turbulence evolves in space and time. Moreover the POD results can be used to build dynamical models for the turbulence, which distinguishes them from many other approaches. In the following paragraphs we will summarize some recent experimental results from our own laboratory that give clues as to why the POD might provide what the LES needs. (For more details, please consult the original references or George et al.⁴² on which this section is based.)

Johansson et al.⁴⁰ report application of the “slice” POD using rakes of hot wires at various downstream cross sections of the axisymmetric wake behind a disk at a Reynolds number based on diameter and freestream velocity of 2.8×10^4 . Jung et al.³⁹ and Gamard et al.⁴¹ report similar application of the slice POD using 138 hot wires in the axisymmetric jet with nearly top-hat source conditions at source Reynolds numbers ranging from 4×10^4 to 1.57×10^5 . In both experiments the first radial POD mode contains approximately 60% of the resolved streamwise energy (about 40% of the total streamwise energy), and only it will be of interest herein.

Of primary interest is the eigenspectrum of this first POD mode, which shows how the energy of the cross section is distributed with azimuthal mode number m and temporal frequency f , that is, $\lambda^{(1)}(m, f)$. Note that the variable f is considered to be continuous, while m is integer and positive for the eigenspectra considered. The eigenspectra can be integrated over frequency f to obtain the distribution of energy with only the azimuthal mode number m . If this is normalized by the total energy at the cross section, the result is

$$\xi^{(1)}(m) = \frac{\int_0^\infty \lambda^{(1)}(m, f) df}{\sum_{m=0}^M \int_0^\infty \lambda^{(1)}(m, f) df} \tag{26}$$

Eigenspectra as Function of m Only

Figure 10⁴³ shows the downstream evolution of this first azimuthal eigenspectrum $\xi^{(1)}(m)$ for the jet.

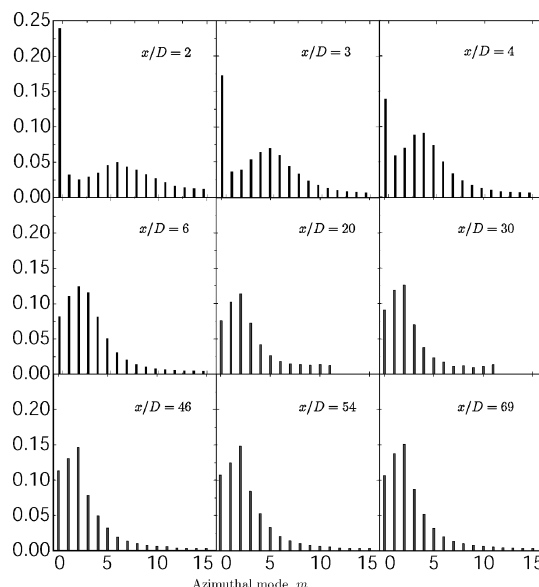


Fig. 10 Energy distribution with azimuthal mode number for the lowest-order POD mode of the axisymmetric turbulent jet (from Gamard⁴³).

For the jet, the azimuthal mode distribution in Fig. 10 at $x/D = 2$ shows a dominant peak at mode 0 and a distribution of energy centered about mode 6. As the distance from the exit plane is increased, mode 0 diminishes, and the center of the distribution moves to lower values, from mode 5 at $x/D = 3$ to only a distribution around mode 2 by $x/D = 6$. After $x/D \approx 6$, the distribution shows no further evolution, coincident with the fact that the mean centerline velocity has approximately reached near similarity behavior (about $x/D \approx 10$). Also the ratio of centerline rms velocity to the mean centerline velocity is constant shortly after this evolution is complete, and the mean velocity profiles and turbulence intensity profiles begin to collapse as well. Obviously the diminishing value of mode 0 and the emer-

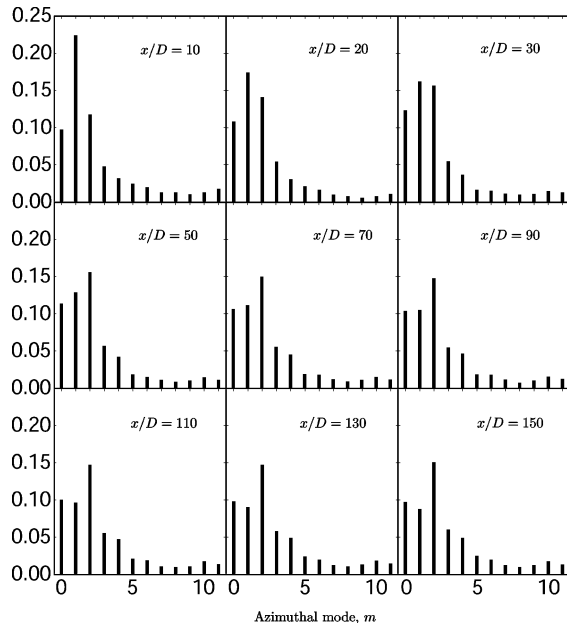


Fig. 11 Energy distribution with azimuthal mode number for the lowest-order POD mode of the axisymmetric disk wake (from Johansson³).

gence of the mode 2 peak both reflect (or are responsible for) the process by which a top-hat profile evolves into a self-preserving jet.

Figure 11 shows a similar azimuthal mode evolution for the axisymmetric wake behind a disk. For the near wake, at $x/D = 10$ mode 1 dominates, but by $x/D = 30$ the energy in mode 2 is nearly equal to that in mode 1. By $x/D = 50$, mode 2 dominates, as it does for all downstream positions.

Like the jet, the emergence of this mode-2 dominance corresponds also to the emergence of the similarity state, particularly evident in the normalized turbulence intensity, which does not approach a constant until about $x/D = 50 - 70$. The implications of this for attempts to study axisymmetric wakes are profound because most attempts seldom measure much beyond this point as a result of the extremely low turbulence intensities and limited wind-tunnel lengths.

Eigenspectra as Functions of m and f

Experimentally f is the frequency (or temporal variation) observed by the measuring apparatus. For the wake where $u'/U < 10\%$, Taylor's hypothesis is certainly valid, at least for all but the very lowest frequencies, and so we can examine how these spatial decompositions evolve downstream.

Figure 12 shows three-dimensional plots (for positive m and f) of the first eigenspectrum $\lambda^{(1)}(m, f, x)$, for the disk wake at $x/D = 30, 50, 90,$ and 150 . The most striking feature is the clear separation of the frequency content of the various modes. Only mode 1 has a peak at a nonzero frequency. The other eigenspectra (of which mode 2 is predominant) all resemble the usual broadband one-dimensional spectra of turbulence which peak at zero frequency (usually caused by aliasing from the unresolved directions). The eigenspectra have not been normalized, so that their heights decay downstream as the wake itself decays. But even from just these four plots it is obvious that mode 1 dies more quickly than the other modes and especially mode 2. In fact, the reason for the behavior of the preceding normalized azimuthal mode number plots (Fig. 11) is clearly not that mode 2 is increasing its contribution, but that mode 1 is fading more rapidly.

Figure 13 shows plots of the total energy and mode 1 alone as a function of frequency for the same downstream positions. Most striking is that the peak frequency of the band, which contains most

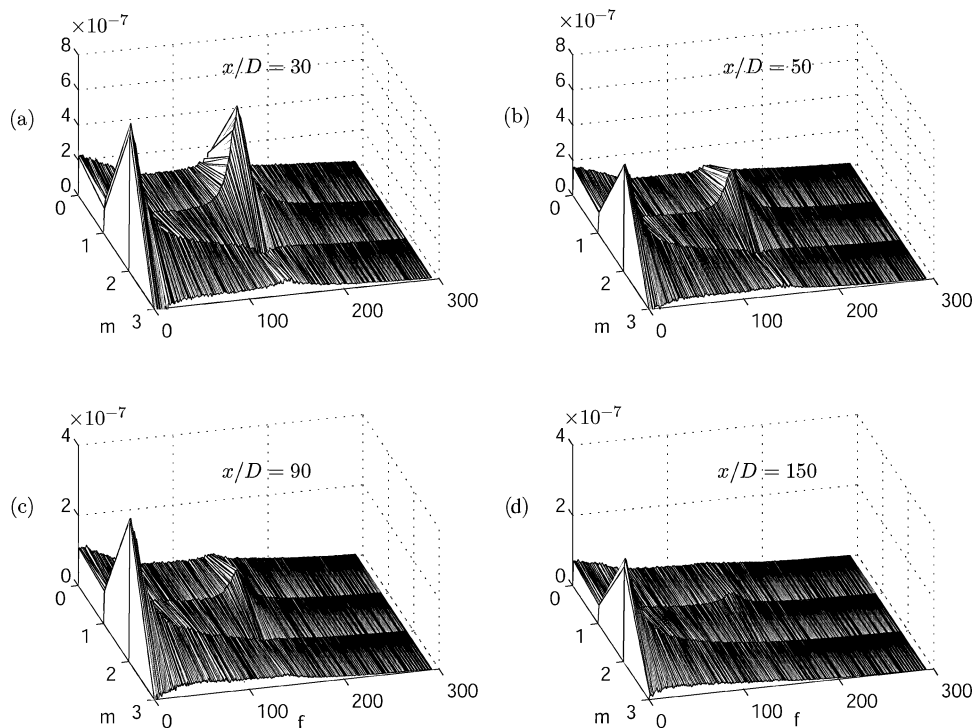


Fig. 12 Eigenspectra of first POD mode as function of frequency, azimuthal mode number, and downstream distance $\lambda^{(1)}(f, m, x)$ for the disk wake at $x/D = 30, 50, 90,$ and 150 diameters downstream (from Johansson³).

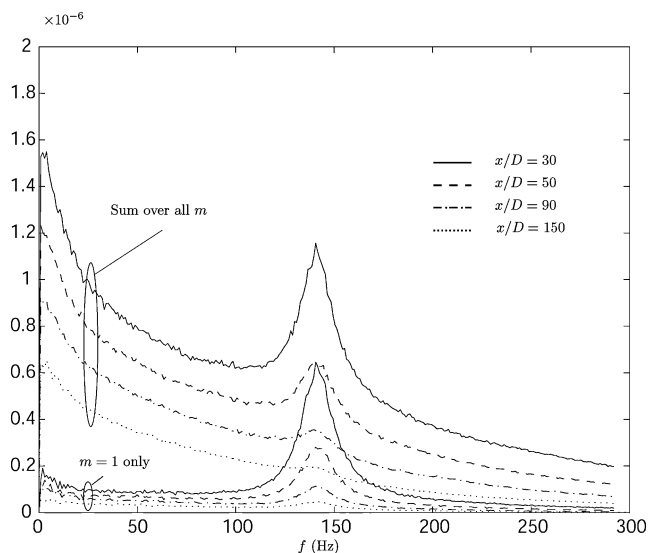


Fig. 13 Total energy (all azimuthal modes) and mode 1 only as a function of frequency at $x/D = 30, 50, 90,$ and 150 (from Johansson³).

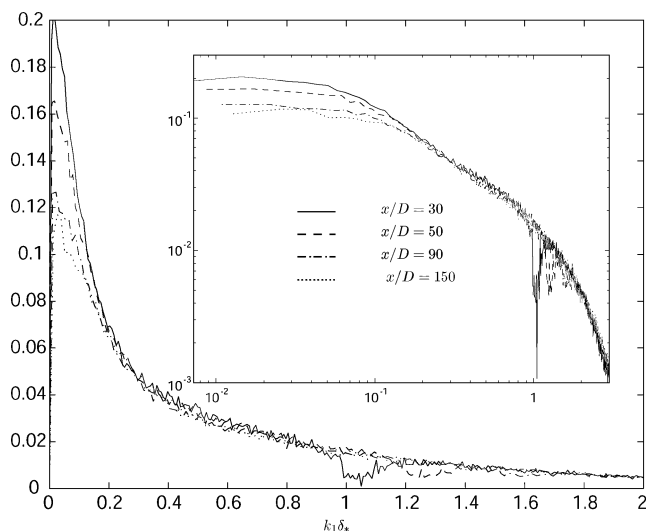


Fig. 14 Azimuthal mode 2 only at $x/D = 30, 50, 90,$ and 150 normalized by the energy remaining AFTER the energy from azimuthal mode 1 is removed (from Johansson³). These data have been plotted as wave-number data using Taylor’s hypothesis. Note especially the apparent suppression of mode 2 at the peak frequency of mode 1 for $x/D = 30$.

of the energy for mode 1, does not evolve downstream, but is fixed. Moreover its contribution to the total energy is clearly diminishing downstream, as just noted. Thus the primary contribution of mode 1 clearly does not scale in local shear-layer variables, but is instead determined only by the Strouhal number of the wake generator itself. It seems apparent that the primary contribution to mode 1 has been convected in from the near wake and is virtually independent of the local shear layer of the wake.

By contrast, the behavior of mode 2 is quite different. Figure 14 shows mode 2 normalized by the energy remaining after the energy from mode 1 is removed. These data have been plotted as wave-number spectra using Taylor’s frozen field hypothesis. Note first of all the remarkable notch in mode 2 (all of the way to zero!) for the position closest to the disk at exactly the frequency where mode 1 is dominant. Clearly mode 1 is suppressing the development of mode 2 at the dominant frequency. As the wake develops downstream, this notch fills in, and except for the very lowest wave numbers (for which Taylor’s hypothesis is of doubtful validity) these data collapse wonderfully in shear-layer variables. Thus, once the contribution of mode 1 has been removed, the rest of the turbulence behaves exactly

as might be expected from an equilibrium similarity wake. This is certainly not the case if mode 1 is not removed, which explains the frustrations of many authors in trying to explain their measurements for this flow.

One additional observation can be made. There is a very interesting problem presented by the lack of collapse of the spectra for mode 2 at very low wave numbers (or more properly, very low frequencies). These very low frequencies (or perhaps large scales) clearly satisfy Townsend’s idea of the large eddies. They contain about 5–10% of the energy and do not appear to interact with the main motion. Interestingly, if these data are not normalized with wave numbers, but simply by the energy present at all mode numbers with mode 1 removed, they collapse without any scaling of the frequency axis at all. So what is their role, if any? This is not at all clear as of this writing. One possibility is that they simply slowly warp and twist the mean flow. If so, this could account for the remarkably high local turbulence intensity for this flow for which at the centerline $u'/(U_\infty - U) \approx 130\%$! In effect, it appears the mean profile is simply being moved around by this very large and slow modulation. There is some evidence for this in the azimuthally averaged instantaneous DNS profiles of Johansson et al.²

Several things are clear from the preceding. First, the near-wake structure (mostly azimuthal mode 1) can persist far downstream and considerably complicate a simple scaling analysis. Second, it appears that this transient structure can interact with the structures that eventually dominate the far field. In particular it appears to suppress them early and possibly modulate them later. If so, then it is reasonable to guess that different upstream conditions might interact in different ways. Perhaps it is this interaction that sets the stage for the final asymptotic state.

We have raised more questions than we have answered. Clearly we will not know the answers until more detailed information is available, and dynamical models can be constructed. LES (especially together with the POD) can play an important role in this development, especially given the low-Reynolds-number limitations of DNS and the difficulty of experiments.

Summary

The evidence for the role of initial (or upstream) conditions has been briefly reviewed and shown to be consistent with a properly done equilibrium similarity analysis. Moreover, from the same analysis it was possible to show why the traditional view of asymptotic independence has arisen. In particular, the mean velocity profile and properly scaled Reynolds-stress profile for the axisymmetric wake were shown to be independent of all upstream effects. By contrast, initial condition (and upstream) conditions appear to control the growth rate and scale parameters and the other moment profiles. Similar considerations apply to many other canonical flows.

It was further noted that single-point (RANS) gradient-based turbulence models appear to be fundamentally flawed in that the effects of the initial conditions appear in the coefficients. Thus even if the models have the right functional dependence, the asymptotic state is determined by the particular set of parameters used, and no universal set is possible. LES, on the other hand, appears to retain the necessary physics, whatever it might be.

Finally, some recent POD studies were reviewed to illustrate how upstream conditions might interact with the developing turbulence and permanently modify it. It remains to be seen if dynamical systems and stability models can account for this behavior. Regardless, it appears that LES can be used as an important tool for these studies (perhaps together with the POD), if careful attention is paid to the importance and sensitivity to initial and boundary conditions.

References

- ¹Cannon, S. C., “Large-Scale Structures and the Spatial Evolution of Wakes Behind Axisymmetric Bluff Bodies,” Ph.D. Dissertation, Dept. of Aerospace and Mechanical Engineering, Univ. of Arizona, Tucson, AZ, 1991.
- ²Johansson, P. B. V., George, W. K., and Gourlay, M. J., “Equilibrium Similarity, Effects of Initial Conditions and Local Reynolds Number

- on the Axisymmetric Wake," *Physics of Fluids A*, Vol. 15, No. 3, 2003, pp. 603–617.
- ³Johansson, P. B. V., "The Axisymmetric Turbulent Wake," Ph.D. Dissertation, Dept. of Thermo and Fluid Dynamics, Chalmers Univ. of Technology, Gothenburg, Sweden, 2002.
- ⁴Gourlay, M. J., Arendt, S. C., Fritts, D. C., and Werne, J., "Numerical Modeling of Initially Turbulent Wakes with Net Momentum," *Physics of Fluids A*, Vol. 13, 2001, pp. 3783–3802.
- ⁵Wynanski, I., Champagne, F., and Marasli, B., "On the Large-Scale Structures in Two-Dimensional Small-Deficit, Turbulent Wakes," *Journal of Fluid Mechanics*, Vol. 168, 1986, pp. 31–71.
- ⁶Grinstein, F. F., Glauser, M. M., and George, W. K., "Vorticity in Jets," *Fluid Vortices*, edited by S. Greene, Kluwer, Amsterdam, 1995, pp. 65–94.
- ⁷Grinstein, F., "Vortex Dynamics and Entrainment in Rectangular Free Jets," *Journal of Fluid Mechanics*, Vol. 437, 2001, pp. 69–101.
- ⁸Ghosal, S., and Rogers, M. M., "A Numerical Study of Self-Similarity in a Turbulent Plane Wake Using Large-Eddy Simulation," *Physics of Fluids*, Vol. 9, No. 6, 1997, pp. 1729–1739.
- ⁹Boersma, G. J., Brethouwer, G., and Nieuwstadt, F. T. M., "A Numerical Investigation of the Effect of the Inflow Conditions on the Self-Similar Region of a Round Jet," *Physics of Fluids*, Vol. 10, No. 4, 1998, pp. 899–909.
- ¹⁰Mi, J., Nobis, D. S., and Nathan, G., "Influence of Jet Exit Conditions on the Passive Scalar Field of an Axisymmetric Free Jet," *Journal of Fluid Mechanics*, Vol. 432, 2001, pp. 91–125.
- ¹¹Slessor, M. D., Bond, C. L., and Dimotakis, P. E., "Turbulent Shear-Layer Mixing at High Reynolds Numbers: Effects of Inflow Conditions," *Journal of Fluid Mechanics*, Vol. 376, 1998, pp. 115–138.
- ¹²George, W. K., Abrahamsson, H., Eriksson, J., Karlsson, R. I., Löfdahl, L., and Wosnik, M., "A Similarity Theory for the Turbulent Plane Wall Jet Without External Stream," *Journal of Fluid Mechanics*, Vol. 425, 2000, pp. 367–411.
- ¹³Castillo, L., and George, W. K., "Similarity Analysis of Turbulent Boundary Layers with Pressure Gradient: Outer Flow," *AIAA Journal*, Vol. 39, No. 1, 2001, pp. 41–47.
- ¹⁴Castillo, L., and Johansson, T. G., "The Effects of Upstream Conditions on a Low Reynolds Number Turbulent Boundary Layer with Zero Pressure Gradient," *Journal of Turbulence*, Vol. 3, 2002, p. 31.
- ¹⁵George, W. K., "The Self-Preservation of Turbulent Flows and Its Relation to Initial Conditions and Coherent Structures," *Advances in Turbulence*, edited by W. K. George and R. E. A. Arndt, Hemisphere, New York, 1989, pp. 1–42.
- ¹⁶George, W. K., "Some New Ideas for Similarity of Turbulent Shear Flows," *Turbulence, Heat and Mass Transfer I*, edited by K. Hanjalic and J. C. F. Pereira, Begell House, New York, 1995, pp. 24–49.
- ¹⁷Moser, R. D., Rogers, M. M., and Ewing, D. W., "Self-Similarity of Time-Evolving Plane Wakes," *Journal of Fluid Mechanics*, Vol. 367, 1998, pp. 255–289.
- ¹⁸Rogers, M. M., "The Evolution of Strained Turbulent Plane Wakes," *Journal of Fluid Mechanics*, Vol. 463, 2002, pp. 53–120.
- ¹⁹George, W. K., and Castillo, L., "Zero-Pressure-Gradient Turbulent Boundary Layer," *Applied Mechanics Reviews*, Vol. 50, No. 12, 1997, pp. 689–729.
- ²⁰George, W. K., "The Decay of Homogeneous Isotropic Turbulence," *Physics of Fluids A*, Vol. 4, No. 7, 1992, pp. 1492–1509.
- ²¹George, W. K., and Gibson, M. M., "The Self-Preservation of Homogeneous Shear Flow Turbulence," *Experiments in Fluids*, Vol. 13, 1992, pp. 229–238.
- ²²Ewing, D., "On Multi-Point Similarity Solutions in Turbulent Free-Shear Flows," Ph.D. Dissertation, Dept. of Mechanical and Aerospace Engineering, State Univ. of New York, Buffalo, NY, May 1995.
- ²³Ewing, D., and George, W. K., "Similarity Analysis of the Two-Point Velocity Correlation Tensor in the Turbulent Axisymmetric Jet," *Turbulence, Heat and Mass Transfer I*, edited by K. Hanjalic and J. C. F. Pereira, Begell House, New York, 1995, pp. 49–56.
- ²⁴de Bruyn Kops, S., and Riley, J., "Direct Numerical Simulation of Laboratory Experiments in Isotropic Turbulence," *Physics of Fluids A*, Vol. 10, 1999, pp. 2125–2127.
- ²⁵Wang, H., and George, W. K., "The Integral Scale in Isotropic Turbulence," *Journal of Fluid Mechanics*, Vol. 459, 2002, pp. 429–443.
- ²⁶Wray, A., "Decaying Isotropic Turbulence," AGARD, Advisory Rept. 345, 1998, pp. 63, 64.
- ²⁷Comte-Bellot, G., and Corrsin, S., "The Use of a Contraction to Improve the Isotropy of Grid-Generated Turbulence," *Journal of Fluid Mechanics*, Vol. 25, 1966, pp. 657–682.
- ²⁸Comte-Bellot, G., and Corrsin, S., "Simple Eulerian Time Correlation of Full- and Narrow-Band Velocity Signals in Grid-Generated, 'Isotropic' Turbulence," *Journal of Fluid Mechanics*, Vol. 48, 1971, pp. 273–337.
- ²⁹George, W. K., and Wang, H., "The Spectral Transfer in Isotropic Turbulence," *IUTAM Symposium on Reynolds Number Scaling in Turbulent Flow*, edited by A. J. Smits, Kluwer, Amsterdam, 2002.
- ³⁰Helland, K. N., van Atta, C. W., and Stegun, G. R., "Spectral Energy Transfer in High Reynolds Number Turbulence," *Journal of Fluid Mechanics*, Vol. 79, 1972, pp. 337–359.
- ³¹Wray, A., and Mansour, N. N., "Decay of Isotropic Turbulence at Low Reynolds Number," *Physics of Fluids A*, Vol. 6, No. 2, 1994, pp. 808–814.
- ³²Taulbee, D. B., "Reynolds Stress Models Applied to Turbulent Jets," *Advances in Turbulence*, edited by W. K. George and R. E. A. Arndt, Hemisphere, New York, 1989, pp. 39–73.
- ³³Grinstein, F., "Open Boundary Conditions in the Simulation of Subsonic Turbulent Shear Layers," *Journal of Computational Physics*, Vol. 105, pp. 42–55.
- ³⁴Druault, P., Lareau, S., Bonnet, J. -P., Coiffet, E., Delville, J., Lamballais, E., Largeau, J. F., and Perret, L., "Generation of Three-Dimensional Turbulent Inlet Conditions for Large-Eddy Simulation," *AIAA Journal*, Vol. 42, No. 3, 2004, pp. 447–456.
- ³⁵Delville, J., Ukeiley, L., Cordier, L., Bonnet, J. P., and Glauser, M. N., "Examination of Large-Scale Structures in a Turbulent Plane Mixing Layer. Part I. Proper Orthogonal Decomposition," *Journal of Fluid Mechanics*, Vol. 391, 1999, pp. 91–122.
- ³⁶Citriniti, J. C., and George, W. K., "Reconstruction of the Global Velocity Field in the Axisymmetric Jet Mixing Layer Utilizing the Proper Orthogonal Decomposition," *Journal of Fluid Mechanics*, Vol. 418, 2000, pp. 137–166.
- ³⁷Gordeyev, S., and Thomas, F. O., "Coherent Structure in the Turbulent Planar Jet. Part 1. Extraction of Proper Orthogonal Decomposition Eigenmodes and Their Similarity," *Journal of Fluid Mechanics*, Vol. 414, 2000, pp. 145–194.
- ³⁸Ukeiley, L., Cordier, L., Manceau, R., Delville, J., and Glauser, M. N., "Examination of Large-Scale Structures in a Turbulent Plane Mixing Layer. Part 2. Dynamical Systems Model," *Journal of Fluid Mechanics*, Vol. 441, 2001, pp. 67–108.
- ³⁹Jung, D., Gamard, S., George, W. K., and Woodward, S. H., "Downstream Evolution of the Most Energetic POD Modes in the Mixing Layer of a High Reynolds Number Axisymmetric Jet," *Turbulent Mixing and Combustion, Proceedings of the IUTAM Symposium*, edited by A. Pollard and S. Candel, Kluwer, Amsterdam, 2002, pp. 23–32.
- ⁴⁰Johansson, P. B. V., George, W. K., and Woodward, S., "Proper Orthogonal Decomposition of an Axisymmetric Turbulent Wake Behind a Disk," *Physics of Fluids A*, Vol. 14, No. 6, 2002, pp. 2508–2514.
- ⁴¹Gamard, S., George, W. K., Jung, D., and Woodward, S., "Application of a Slice Proper Orthogonal Decomposition to the Far Field of an Axisymmetric Turbulent Jet," *Physics of Fluids A*, Vol. 14, No. 6, 2002, pp. 2515–2522.
- ⁴²George, W. K., Johansson, P., and Gamard, S., "How Has the Study of Coherent Structures Contributed to Our Understanding of Turbulent Free Shear Flows?," Joint US–European Fluids Engineering Conf., ASME Paper FEDSM 2002-31408, July 2002.
- ⁴³Gamard, S., "The Axisymmetric Jet," Ph.D. Dissertation, Dept. of Thermo and Fluid Dynamics, Chalmers Univ. of Technology, Gothenburg, Sweden, June 2002.

F. Grinstein
Guest Editor